Reading off gravitational radiation waveforms in numerical relativity calculations: Matching to linearized gravity

Andrew M. Abrahams
Department of Astronomy and National Center for Supercomputing Applications, University of Illinois, Urbana, Illinois 61801

Charles R. Evans
Theoretical Astrophysics 130-33, California Institute of Technology, Pasadena, California 91125
(Received 31 August 1987)

Two methods are described, both based on the use of multipole moments in linearized gravity, to read off gravitational radiation waveforms during numerical relativity simulations. In the first, matching is made at a finite radius in the weak-field exterior of a strong-field source to an analytic *template* developed via an infinitesimal gauge transformation from a general solution to the vacuum weak-field equations. The matching procedure allows the asymptotic waveforms to be separated from the confusing influences of the source's (e.g., black hole, neutron star, collapsing stellar core) stationary moments, the wave's near-zone field, and gauge dependencies in the metric. This is achieved by computing the multipole-moment amplitudes of the gravitational field with a set of surface integrals of the metric over one (or more) coordinate two-sphere(s). The two-surface(s) need not be placed far out in the local wave zone, nor does the method require the existence of a deep near zone (i.e., the source need not be slow motion). The procedure is demonstrated through its application to two standard axisymmetric numerical relativity gauges (quasi-isotropic and radial). The second matching approach uses a surface integral over components of the Riemann tensor to eliminate gauge effects. The near-zone field is separated off as in the previous method. This latter technique may be applicable to problems in any gauge.

I. INTRODUCTION

This is the first of several papers in which we will discuss the best strategy for reading off gravitational radiation waveforms from numerical data available at finite radii in spacelike, asymptotically flat numerical relativity calculations employing the Arnowitt-Deser-Misner[1,2] (ADM), or $3+1$, formalism. In this paper we give two procedures for reading off waveforms based on comparing numerical values for the metric with solutions to vacuum linearized gravity. The first is a matching procedure which allows gauge and near-zone effects in the metric to be identified and then separated from the asymptotic radiation waveform. The second prescription avoids gauge effects through use of the Riemann tensor and then performs a similar separation of radiation and near-zone field.

To make these terms precise, *asymptotic radiation* refers to the part of the metric expansion in linearized theory with the form $I_{lm}^{(l)}/r$ (where I_{lm} is the lth-order multipole moment and the superscript represents derivatives with respect to retarded time) and *near-zone field* refers to higher-order terms, such as $I_{lm}^{(l-1)}/r^2$, in the vacuum wave solution that are nonradiative. Gauge conditions which derive from global integrations (parabolic or elliptic) produce additional gauge terms in the metric expansion which, although vanishing at infinity, can be important at finite radii.

The first of our two matching techniques is applied to two spatial gauges (quasi-isotropic and radial) currently employed in numerical relativity calculations. The second method, based on the use of the Riemann tensor, is likely to be applicable in any gauge, though it provides less total information.

Matching techniques based on linearized gravity will only be effective for asymptotically flat spacetimes with certain restrictions on their radiative properties. It is sufficient to require that the objects radiating gravitational waves (e.g., black holes, neutron stars, collapsing stellar cores) be isolated and not radiate away more than a few percent of their rest energy in one characteristic wave period. In this circumstance, approximately stationary mass and angular momentum moments will exist and the emerging radiation will be sufficiently weak as to have negligible nonlinear interaction with itself. Nonlinear coupling between the curved background and the emerging wave (the tails) can be reduced in importance by placing the wave extraction two-surface at a sufficiently large value of r/M (say, ~ 30). The cumulative phase shifts due to the curved background are essentially unobservable and negligible in practical numerical calculations (cf. Thorne's[3] discussion of the split of spacetime around a source into a near zone, a local wave zone, and a distant wave zone; numerical relativity calculations deal with the near zone and local wave zone). For isolated sources that radiate less than a few percent of their mass in one period the most important effects hindering the determination of the waveform are *linear* ones: (1) global linear distortions of the metric components (shearing of the extraction two-surface) due to

dynamic gauge effects and (2) the contribution of the wave's own (linear) nonradiative near-zone field at nonnegligible values of λ/r. Most sources of astrophysical significance, e.g., stellar core collapse, stellar collisions, black-hole formation, collapse of a relativistic star cluster, radiate weakly enough that matching to linearized gravity provides a reasonable first approximation.

The approach we take is to utilize not only a full numerical solution for the strong-field region but also to make use of *analytic techniques* in the surrounding weak-field region so as to (1) aid in interpreting the numerical results and their accuracy, (2) make the numerical computation more efficient, and (3) allow imposition of more accurate boundary conditions. We view this as obligatory; no numerical relativity gauge proposed to date provides metric components or "radiative" variables that are free of the above-mentioned global, time-dependent gauge effects. In any case, the gravitational radiation at a finite radius is affected by the wave's near-zone field regardless of which gauge is chosen. One might ask, why not take an extremely large radius for the outer boundary where all such effects will be greatly diminished? This can be done in one-dimensional (1D) (spherical) calculations since the exterior gravitational field contains only pure power-law dependencies and an exponentially graded mesh can be employed. But in higher dimensions the emitted gravitational waves set a fixed length scale in the weak-field exterior region that requires an upper limit on radial zone size (e.g., $\Delta r \lesssim \lambda/50$) (Ref. 4) and therefore a cost-governed upper limit on the outer boundary radius.

One alternative, in the context of spacelike numerical calculations, would be to use a time-slicing condition which forces the slices to tend asymptotically to outgoing null surfaces[5] (constant mean curvature slices), allowing the radial coordinate to be compactified. Another possibility is to abandon the spacelike approach altogether and perform the evolution on characteristic, or null, hypersurfaces.[6] Unfortunately, the use of the former gauge has not yet been attempted for radiating spacetimes and the latter approaches are not as highly developed for two or three spatial dimensions as the spacelike schemes.

Smarr[7] gave several formulas, based on curvature or connection derived quantities, thought to be useful in deriving the *energy loss* due to radiation. Smarr and York[8] have also discussed a "radiation gauge" that they argue cancels most of the pure-gauge distortion in the metric that affects identifying radiation. Closer to the spirit of our work is the analysis of Bardeen,[9] who looked at the extraction of actual waveforms from the metric and examined the asymptotic dependence of several gauges in a way similar to that done in this paper. In addition, Schutz[10] has also recently given an approximate waveform extraction technique which computes surface integrals over projected components of the Riemann tensor. His method requires the existence of at least a narrow weak-field near zone, and this may be difficult to obtain in certain numerical applications, especially for sources that produce broadband bursts of radiation.

A significant advance made in the last five years was to identify special dynamical, or radiative, variables for numerical evolution (e.g., η and λ plus ξ and $K^{\theta}{}_{\phi}$ in quasi-isotropic gauge[4] and η and K_{+} plus ξ and K_{-} in radial gauge,[11] i.e., special combinations of metric components and extrinsic curvature components). These variables yield the asymptotic waveforms directly as $r \to \infty$ and aid in reading off the radiation at large, but finite, radii. Yet, as we show in this paper, this procedure, while a major advance, is only partly satisfactory. Basically, the dynamical metric variables are contrived so as to eliminate the mass monopole from their asymptotic dependence. Even so, at any finite radius the exterior dependence of these variables still involves a mixture of the radiation, the near-zone field, and gauge effects. Hence, they cannot be used blindly as a measure of the asymptotic waveform without first accounting for and removing these other effects.

The intention of the work described here is to develop waveform extraction techniques to account for these effects and allow one to read off the gravitational waveforms in numerical relativity calculations. We use linearized gravity to produce a general weak-field solution and then employ infinitesimal transformations to particular gauges to construct *matching templates.* The matching templates are expressed in terms of multipole moments. Then numerical moments are derived as functions of time by surface integrals at one or more large but finite radii. By matching these amplitudes to the analytic template, sufficient information is available to determine the waveforms, stationary mass moment, gauge terms, and near-zone field. Consistency of the matching can be checked by comparing results obtained at several different extraction radii. As part of this procedure, the asymptotic waveforms are separated from the near-zone field by performing integrations over the past timelike cylinder swept out by the matching two-surface. This allows the matching to be accomplished anywhere in the transition zone (i.e., for any value of λ/r on the matching two-surface), provided the field is sufficiently weak (e.g., $M/r \lesssim$ a few percent). It is important to keep in mind that at this level of approximation errors in the waveform will be comparable in size to finite difference truncation errors.

This work was influenced by the recent efforts of Anderson and Hobill.[12] Their approach to constructing a matching template is ultimately more complete than ours: they use Bondi null coordinates to construct a vacuum solution expansion that can contain both a curved background and the nonlinearities of the wave coupling to itself and the background. Our alternative use of linearized gravity to provide a matching template is motivated by (1) numerical experience which has indicated the above-mentioned linear gauge and near-zone effects to be the dominant impediments, at $r \gtrsim 30M$, to reading off waveforms, and (2) the practical desire to see how the complete procedure of matching the template to data is to be accomplished. As we show, even the linear analysis is somewhat involved, though rather simple to implement. Experience gained with the method described here should guide the development of more ela-

borate matching schemes, which may, in some applications, allow the matching radius to be pushed in deeper to $r \ll 30M$.

The outline of the paper is as follows. In Sec. II we derive a useful form for the general solution to the vacuum equations of linearized gravity using tensor spherical harmonics. Our solution is written in terms of the Lorentz gauge (using a subgauge specialization due to Thorne). This solution is of interest in its own right (e.g., to provide wave solutions for numerical tests). In Sec. III we combine it with infinitesimal gauge transformations to form matching templates for use with two gauges currently known to be suitable for numerical calculations of axisymmetric collapse: quasi-isotropic gauge and radial gauge. The reader interested in the gravitational radiation extraction techniques *per se* can skip Secs. II and III and turn to Secs. IV and V. Section IV details how the matching templates are used to read off radiation waveforms and to obtain other useful information while Sec. V gives an alternate way of reading off waveforms based on a surface integral of the Riemann tensor. In Sec. VI we summarize the principal results derived in this paper, discuss the expected realm of applicability of the extracted waveforms, and mention briefly several issues to be dealt with in further detail in a subsequent paper. An Appendix is given that contains a number of computational details and notation used throughout the paper.

II. LINEARIZED GRAVITY

We start by finding a general solution in linearized theory in a suitable gauge for the vacuum, weak, exterior gravitational field of an isolated source. In linearized theory, the background metric is taken to be the Minkowskii metric $\eta_{\alpha\beta}$ and the true metric differs from $\eta_{\alpha\beta}$ by a perturbation $h_{\alpha\beta}$:

$$g_{\alpha\beta}=\eta_{\alpha\beta}+h_{\alpha\beta}. \tag{1}$$

We use the notation that greek indices run from 0 to 3 and latin indices from 1 to 3. Geometrized units are used ($G=c=1$) and the metric signature is $(-1,+1,+1,+1)$. An often more useful quantity is the trace-reversed perturbation,[13] or gravitational field, $\bar{h}_{\alpha\beta}$:

$$\bar{h}_{\alpha\beta}=h_{\alpha\beta}-\tfrac{1}{2}\eta_{\alpha\beta}\,\eta^{\gamma\delta}\,h_{\gamma\delta}, \tag{2}$$

where indices on the perturbed metric are raised and lowered with $\eta_{\alpha\beta}$.

In the Lorentz gauge $\bar{h}^{\alpha\beta}{}_{|\beta}=0$, the covariant form of the linearized equations is

$$\partial_t \bar{h}_{\alpha t}=\nabla_k \bar{h}_{\alpha k}, \tag{3}$$

$$\Box\bar{h}_{\alpha\beta}\equiv-\partial_t^2\bar{h}_{\alpha\beta}+\nabla_k\nabla_k\bar{h}_{\alpha\beta}=0. \tag{4}$$

We use spherical orthonormal components unless explicitly noted otherwise. In addition, repeated latin down indices are to be summed as though a δ_{ij} were present, and vertical bar and ∇ denote, respectively, four-dimensional and spatial flat-space covariant derivatives along the spherical orthonormal basis

$$\mathbf{e}_\alpha=\left[\frac{\partial}{\partial t},\frac{\partial}{\partial r},\frac{1}{r}\frac{\partial}{\partial\theta},\frac{1}{r\sin\theta}\frac{\partial}{\partial\phi}\right]. \tag{5}$$

The linearized field equations (4) are scalar, vector, and tensor wave equations for $\bar{h}_{tt}$, $\bar{h}_{ti}$, and $\bar{h}_{ij}$. Solutions can be written down in terms of pure-orbit tensor spherical harmonics[3] (eigenfunctions of the orbital angular momentum operator $\mathbf{L}^2$) and solutions to the radial wave equation (see the Appendix). The most general such solution is

$$\bar{h}_{tt}=\sum_{l=0}^{\infty}\sum_{m=-l}^{+l}\{\mathcal{A}^{(l)}_{lm}(t-\epsilon r)\}_l Y^{lm}, \tag{6a}$$

$$\bar{h}_{ti}=\sum_{l=1}^{\infty}\sum_{m=-l}^{+l}[\{\mathcal{B}^{(l-1)}_{lm}(t-\epsilon r)\}_{l-1}Y_i^{l-1,lm}+\{\mathcal{C}^{(l)}_{lm}(t-\epsilon r)\}_l Y_i^{l,lm}]+\sum_{l=0}^{\infty}\sum_{m=-l}^{+l}\{\mathcal{D}^{(l+1)}_{lm}(t-\epsilon r)\}_{l+1}Y_i^{l+1,lm}, \tag{6b}$$

$$\begin{aligned}\bar{h}_{ij}=&\sum_{l=2}^{\infty}\sum_{m=-l}^{+l}[\{\mathcal{E}^{(l-2)}_{lm}(t-\epsilon r)\}_{l-2}T_{ij}^{2\ l-2,lm}+\{\mathcal{F}^{(l-1)}_{lm}(t-\epsilon r)\}_{l-1}T_{ij}^{2\ l-1,lm}]\\&+\sum_{l=1}^{\infty}\sum_{m=-l}^{+l}[\{\mathcal{G}^{(l)}_{lm}(t-\epsilon r)\}_l T_{ij}^{2\ l,lm}+\{\mathcal{H}^{(l+1)}_{lm}(t-\epsilon r)\}_{l+1}T_{ij}^{2\ l+1,lm}]\\&+\sum_{l=0}^{\infty}\sum_{m=-l}^{+l}[\{\mathcal{I}^{(l+2)}_{lm}(t-\epsilon r)\}_{l+2}T_{ij}^{2\ l+2,lm}+\{\mathcal{H}^{(l)}_{lm}(t-\epsilon r)\}_l T_{ij}^{0\ l,lm}].\end{aligned} \tag{6c}$$

Equation (6) is similar to Thorne's[3] Eq. (8.4), but is given here in terms of pure-orbit harmonics rather than symmetric trace-free (STF) harmonics. Here and throughout this paper we follow Burke[14] in using curly brackets to denote solutions of the radial wave equation. These solutions are functionals of derivatives (indicated by superscripts in

parentheses) of general functions of advanced ($\epsilon=-1$) or retarded ($\epsilon=+1$) time and have orbital angular momentum $l'=l\pm2,l\pm1,l$ (l represents the total angular momentum). Properties of these solutions are given in the Appendix, as is the notation for tensor spherical harmonics.

The Lorentz gauge condition (3) relates the ten amplitudes by four conditions [similar to Thorne's[3] Eq. (8.5)]:

$$\{\mathcal{A}_{lm}^{(l+1)}\}_l+\epsilon\left[\frac{l}{2l+1}\right]^{1/2}\{\mathcal{B}_{lm}^{(l)}\}_l-\epsilon\left[\frac{l+1}{2l+1}\right]^{1/2}\{\mathcal{D}_{lm}^{(l+2)}\}_l=0, \tag{7a}$$

$$\{\mathcal{B}_{lm}^{(l)}\}_{l-1}+\epsilon\left[\frac{l-1}{2l-1}\right]^{1/2}\{\mathcal{E}_{lm}^{(l-1)}\}_{l-1}-\epsilon\left[\frac{(2l+3)(l+1)}{6(2l-1)(2l+1)}\right]^{1/2}\{\mathcal{G}_{lm}^{(l+1)}\}_{l-1}-\epsilon\left[\frac{l}{3(2l+1)}\right]^{1/2}\{\mathcal{K}_{lm}^{(l+1)}\}_{l-1}=0, \tag{7b}$$

$$\{\mathcal{C}_{lm}^{(l+1)}\}_l+\epsilon\left[\frac{l-1}{2(2l+1)}\right]^{1/2}\{\mathcal{F}_{lm}^{(l)}\}_l-\epsilon\left[\frac{l+2}{2(2l+1)}\right]^{1/2}\{\mathcal{H}_{lm}^{(l+2)}\}_l=0, \tag{7c}$$

$$\{\mathcal{D}_{lm}^{(l+2)}\}_{l+1}+\epsilon\left[\frac{l(2l-1)}{6(2l+1)(2l+3)}\right]^{1/2}\{\mathcal{G}_{lm}^{(l+1)}\}_{l+1}-\epsilon\left[\frac{l+2}{2l+3}\right]^{1/2}\{\mathcal{J}_{lm}^{(l+3)}\}_{l+1}+\epsilon\left[\frac{l+1}{3(2l+1)}\right]^{1/2}\{\mathcal{K}_{lm}^{(l+1)}\}_{l+1}=0. \tag{7d}$$

As is well known, imposing the Lorentz gauge does not uniquely fix the form of the solution. Freedom exists to make additional infinitesimal gauge transformations with generators ξ_α provided $\Box\xi_\alpha=0$. If the choice $\mathcal{A}_{lm}=\mathcal{B}_{lm}=\mathcal{C}_{lm}=\mathcal{D}_{lm}=\mathcal{K}_{lm}=0$ is made, the transverse-traceless (TT) form of the solution for $l=2$ described by Teukolsky[15] is obtained.

We prefer a different gauge specialization for the solution. This was derived by Thorne[3] in STF tensor notation; we express the equivalent result here in terms of pure-orbit harmonics. This gauge has a somewhat simpler form which makes it more convenient when dealing with higher l-mode expressions. It also allows for inclusion of the stationary $l=0$ and $l=1$ terms, which TT gauge does not, and it produces simpler infinitesimal gauge transformations to other gauges that we will consider. Thorne makes what amounts to the requirement

$$\mathcal{D}_{lm}=\mathcal{G}_{lm}=\mathcal{K}_{lm}=\mathcal{J}_{lm}=0. \tag{8}$$

This can always be obtained from any solution of the form (6) through an infinitesimal gauge transformation

$$\bar{h}'_{\alpha\beta}=\bar{h}_{\alpha\beta}+\nabla_\alpha\xi_\beta+\nabla_\beta\xi_\alpha-\eta_{\alpha\beta}\nabla_\gamma\xi^\gamma, \tag{9}$$

with the generators

$$\xi_t=\left[-\epsilon\left[\frac{2l+1}{l+1}\right]^{1/2}\{\mathcal{D}_{lm}^{(l)}\}_l+\frac{1}{2}\left[\frac{(2l+1)(2l+3)}{(l+1)(l+2)}\right]^{1/2}\{\mathcal{J}_{lm}^{(l+1)}\}_l\right]Y^{lm}, \tag{10a}$$

$$\xi_i=\left[-\epsilon\left[\frac{3(2l+1)(2l-1)}{2(l+1)(2l+3)}\right]^{1/2}\{\mathcal{G}_{lm}^{(l-1)}\}_{l-1}-\epsilon\tfrac{1}{2}(2l-1)\left[\frac{l}{(l+1)(l+2)(2l+3)}\right]^{1/2}\{\mathcal{J}_{lm}^{(l+1)}\}_{l-1}\right]Y_i^{l-1,lm}$$
$$-\epsilon\left[\frac{2l+1}{2(l+2)}\right]^{1/2}\{\mathcal{H}_{lm}^{(l)}\}_l Y_i^{l,lm}-\epsilon\frac{1}{2}\left[\frac{2l+3}{l+2}\right]^{1/2}\{\mathcal{J}_{lm}^{(l+1)}\}_{l+1}Y_i^{l+1,lm}. \tag{10b}$$

These obviously maintain the Lorentz condition (3) and they in turn imply $\mathcal{K}_{lm}=0$.

We are led by this gauge specialization to a single pair of independent amplitudes for each value of $l\geq2$ (only one moment for $l=0$ and, after placing the center of coordinates at the center of mass, only one for $l=1$). For $l\geq2$ we define a mass moment $\mathcal{I}_{lm}$ with parity $\pi=(-1)^l$ and a current moment $\mathcal{S}_{lm}$ with parity $\pi=(-1)^{l+1}$ by

$$\mathcal{I}_{lm}=\left[\frac{(l+1)(l+2)}{2l(l-1)}\right]^{1/2}\mathcal{A}_{lm},\qquad \mathcal{S}_{lm}=-i\epsilon\left[\frac{2(l+1)}{l-1}\right]^{1/2}\mathcal{C}_{lm}. \tag{11}$$

Our normalization guarantees that the transverse-traceless part of the metric perturbation has the standard asymptotic form

$$h_{ij}^{\mathrm{TT}}=\sum_{l=2}^{\infty}\sum_{m=-l}^{l}\left[\frac{\mathcal{I}_{lm}^{(l)}}{r}T_{ij}^{E2,lm}+\frac{\mathcal{S}_{lm}^{(l)}}{r}T_{ij}^{B2,lm}\right], \tag{12}$$

with the multipole moments $\mathcal{I}_{lm}$ and $\mathcal{S}_{lm}$ giving the two polarization states of the radiation field,[16] expressed in terms of the TT pure-spin tensor harmonics $\mathbf{T}^{E2,lm}$ and $\mathbf{T}^{B2,lm}$. In this Lorentz-Thorne (LT) gauge, the gravitational field then has the form

$$\bar{h}_{tt}=\frac{4M}{r}+\sum_{l=2}^{\infty}\sum_{m=-l}^{+l}\left[\frac{2l(l-1)}{(l+1)(l+2)}\right]^{1/2}\{\mathcal{I}^{(l)}_{lm}\}_l Y^{lm}, \tag{13a}$$

$$\bar{h}_{ti}=-\frac{2}{r^2}\epsilon_{ijk}J_j n_k-\sum_{l=2}^{\infty}\sum_{m=-l}^{+l}\left[\epsilon\left[\frac{2(l-1)(2l+1)}{(l+1)(l+2)}\right]^{1/2}\{\mathcal{I}^{(l)}_{lm}\}_{l-1}Y^{l-1,lm}_i+i\epsilon\left[\frac{l-2}{2(l+2)}\right]^{1/2}\{\mathcal{S}^{(l)}_{lm}\}_l Y^{l,lm}_i\right], \tag{13b}$$

$$\bar{h}_{ij}=\sum_{l=2}^{\infty}\sum_{m=-l}^{+l}\left[\left[\frac{2(2l-1)(2l+1)}{(l+1)(l+2)}\right]^{1/2}\{\mathcal{I}^{(l)}_{lm}\}_{l-2}T^{2\,l-2,lm}_{ij}+i\left[\frac{2l+1}{l+2}\right]^{1/2}\{\mathcal{S}^{(l)}_{lm}\}_{l-1}T^{2\,l-1,lm}_{ij}\right], \tag{13c}$$

where $n_j=x_j/r$ and the stationary mass moment M ($l=0$) and angular momentum J_j ($l=1$) have been explicitly split off. These moments M and J_j are admitted by Eqs. (3) and (4) but only exist for linearized gravity in the vacuum exterior of a material body. In complete vacuum they vanish and the multipole expansion begins at $l=2$.

By transforming back using (2), the metric perturbation becomes

$$h_{tt}=\frac{2M}{r}+\sum_{l=2}^{\infty}\sum_{m=-l}^{+l}\left[\frac{l(l-1)}{2(l+1)(l+2)}\right]^{1/2}\{\mathcal{I}^{(l)}_{lm}\}_l Y^{lm}, \tag{14a}$$

$$h_{ti}=-\frac{2}{r^2}\epsilon_{ijk}J_j n_k-\sum_{l=2}^{\infty}\sum_{m=-l}^{+l}\left[\epsilon\left[\frac{2(l-1)(2l+1)}{(l+1)(l+2)}\right]^{1/2}\{\mathcal{I}^{(l)}_{lm}\}_{l-1}Y^{l-1,lm}_i+i\epsilon\left[\frac{l-1}{2(l+2)}\right]^{1/2}\{\mathcal{S}^{(l)}_{lm}\}_l Y^{l,lm}_i\right], \tag{14b}$$

$$h_{ij}=\delta_{ij}\left[\frac{2M}{r}+\sum_{l=2}^{\infty}\sum_{m=-l}^{+l}\left[\frac{l(l-1)}{2(l+1)(l+2)}\right]^{1/2}\{\mathcal{I}^{(l)}_{lm}\}_l Y^{lm}\right]$$
$$+\sum_{l=2}^{\infty}\sum_{m=-l}^{+l}\left[\left[\frac{2(2l-1)(2l+1)}{(l+1)(l+2)}\right]^{1/2}\{\mathcal{I}^{(l)}_{lm}\}_{l-2}T^{2\,l-2,lm}_{ij}+i\left[\frac{(2l+1)}{l+2}\right]^{1/2}\{\mathcal{S}^{(l)}_{lm}\}_{l-1}T^{2\,l-1,lm}_{ij}\right]. \tag{14c}$$

This is the complete solution to the linearized equations for all l modes.[17] This solution can now be used to construct test waveforms[4] for any order l and m or provide, through infinitesimal gauge transformation, a template for analytic-numerical matching.

In this paper we only detail how gravitational radiation can be read off in two-dimensional applications using several common axisymmetric gauges. However, the approach is likely to be applicable to three-dimensional numerical calculations as well.[18] In axisymmetry we have the simplification $m=0$ in all terms. In addition equatorial plane symmetry is typically also assumed in numerical calculations. This requires that all odd-l mass moments and all even-l current moments vanish. The most important terms to match are the low-order moments; hence, we only take the expansion to include the first two mass moments, $l=0$ (static) and $l=2$, and the first two current moments, $l=1$ (stationary) and $l=3$ (Ref. 19). The dynamical $l=2$ and $l=3$ moments carry partial information on the two polarization states + and $\times$, respectively, of the radiation.

It is important to comment on the choice of truncating the expansion with this number of moments. Even vibrating neutron stars are to a great extent slow-motion sources. For slow-motion sources, the terms in our radiation field (12) are of order of magnitude

$$(h^{\mathrm{TT}}_{ij})_{\text{mass } l\text{-pole}}\sim(M/r)(R/\lambda\!\!\!^{-})^l,$$

$$(h^{\mathrm{TT}}_{ij})_{\text{current } l\text{-pole}}\sim(M/r)(R/\lambda\!\!\!^{-})^{l+1},$$

where M is the source mass, R is its characteristic size, and $\lambda\!\!\!^{-}$ is the characteristic reduced wavelength. Thus, to retain the same level of accuracy in the extraction of the waveforms, we should read off the hexadecapole ($l=4$) mass moment since it is equivalent in size to the octupole ($l=3$) current moment. This can readily be done using the general solution (14) and extending the extraction method described in subsequent sections of this paper. In the present paper we are predominantly interested in detailing how analytic-numerical matching is defined and numerically implemented, and so have chosen to restrict the complexity of the discussion by utilizing only one pair of time varying mass and current moments as examples.

To write simple explicit forms for the metric components in terms of trigonometric functions, or Legendre polynomials, we introduce in this paper the following scaled quadrupole and octupole moments:[20]

$$I=\left[\frac{15}{64\pi}\right]^{1/2}\mathcal{I}_{l=2,m=0},$$
$$S=\left[\frac{105}{64\pi}\right]^{1/2}\mathcal{S}_{l=3,m=0}. \tag{15}$$

Taking $J=(\mathbf{J}\cdot\mathbf{J})^{1/2}$ we now give the complete form of the metric perturbation in terms of these moments and in orthonormal spherical-polar components:

$$h_{tt}=\frac{2M}{r}+\tfrac{2}{3}\{I^{(2)}\}_2P_2, \tag{16a}$$
$$h_{tr}=-\tfrac{4}{3}\epsilon\{I^{(2)}\}_1P_2, \tag{16b}$$
$$h_{t\theta}=2\epsilon\{I^{(2)}\}_1\sin\theta\cos\theta, \tag{16c}$$
$$h_{t\phi}=-\frac{2J\sin\theta}{r^2}+\tfrac{1}{5}\epsilon\{S^{(3)}\}_3\sin\theta(5\cos^2\theta-1), \tag{16d}$$
$$h_{rr}=\frac{2M}{r}+(\tfrac{2}{3}\{I^{(2)}\}_2+\tfrac{4}{3}\{I^{(2)}\}_0)P_2, \tag{16e}$$
$$h_{\theta\theta}=\frac{2M}{r}+\tfrac{2}{3}\{I^{(2)}\}_2P_2+\tfrac{2}{3}\{I^{(2)}\}_0(2-3\cos^2\theta), \tag{16f}$$
$$h_{\phi\phi}=\frac{2M}{r}+\tfrac{2}{3}\{I^{(2)}\}_2P_2-\tfrac{2}{3}\{I^{(2)}\}_0, \tag{16g}$$
$$h_{r\theta}=-2\{I^{(2)}\}_0\sin\theta\cos\theta, \tag{16h}$$
$$h_{r\phi}=-\tfrac{1}{5}\{S^{(3)}\}_2\sin\theta(5\cos^2\theta-1), \tag{16i}$$
$$h_{\theta\phi}=\{S^{(3)}\}_2\sin^2\theta\cos\theta, \tag{16j}$$

where P_2 is the Legendre polynomial. In this gauge the radiative variable η (discussed in Sec. III) is exceedingly simple,

$$\eta=\tfrac{1}{2}(h_{\theta\theta}-h_{\phi\phi})=\frac{I^{(2)}}{r}\sin^2\theta, \tag{17a}$$

compared to its form in the TT gauge:[21]

$$\eta=\left[\frac{I^{(2)}}{r}+2\epsilon\frac{I^{(1)}}{r^2}+3\frac{I}{r^3}+3\epsilon\frac{I^{(-1)}}{r^4}+3\frac{I^{(-2)}}{r^5}\right]\sin^2\theta, \tag{17b}$$

where negative superscripts indicate successive integrals of I (Ref. 22).

III. MATCHING TEMPLATES FOR NUMERICAL RELATIVITY GAUGES

To date no axisymmetric numerical simulations have employed the harmonic gauge condition[23] [full nonlinear generalization of Lorentz gauge, Eq. (3)]. The primary considerations in choosing gauge conditions for numerical applications have been (1) to produce good time slices[24] and (2) to have an algebraically simple three-metric to simplify the form of the Einstein equations that must be finite differenced;[7,11] and harmonic gauge is not good in these respects. Two time-slicing conditions, maximal[24] and polar,[25] have been widely utilized in numerical calculations and two spatial gauge choices have emerged to simplify the three-metric: the quasi-isotropic (QI) gauge[4,7,11,26,27] (also called isothermal[7]) and the radial (RD) gauge.[11] Because these gauges involve global elliptic or parabolic integration to determine the coordinates, the asymptotic gravitational field contains nontrivial time-dependent gauge effects. In this section we will show how these gauge effects, as well as the near-zone field, manifest themselves in the QI and RD gauges.

The QI spatial line element, expressed in terms of spherical-polar coordinates, has the form

$$ds^2=A^2\,(dr^2+r^2\,d\theta^2)+B^2\,r^2\,(\sin\theta\,d\phi+\xi\,d\theta)^2, \tag{18a}$$

which stems from the three coordinate component conditions

$$g_{r\phi}=0, \tag{18b}$$
$$g_{r\theta}=0, \tag{18c}$$
$$g_{\theta\theta}\,g_{\phi\phi}-(g_{\theta\phi})^2=g_{rr}\,g_{\phi\phi}\,r^2. \tag{18d}$$

The line element has been simplified to involve only three independent functions: A, B, and ξ. A more natural set of variables[4,26] is the combinations

$$\phi^6=A^2\,B, \tag{19a}$$
$$\eta=\ln(A/B), \tag{19b}$$

where ϕ is the conformal factor[2] and η is a measure of the anisotropy of the three space. Together, ξ and η provide a pair of suitable dynamical variables. In contrast, the conformal factor ϕ is found on successive time slices by solution of the (elliptic) Hamiltonian constraint.

The RD gauge has a line element, when expressed in terms of spherical-polar coordinates, of the form

$$ds^2=A^2\,dr^2+B^{-2}\,r^2\,d\theta^2+B^2\,r^2\,(\sin\theta\,d\phi+\xi\,d\theta)^2, \tag{20a}$$

where the two coordinate component conditions (18b) and (18c) have been applied as well as a new third condition:

$$g_{\theta\theta}\,g_{\phi\phi}-(g_{\theta\phi})^2=r^4\sin^2\theta, \tag{20b}$$

in place of (18d). This line element similarly contains three independent functions though the metric has been simplified in a different way. Bardeen and Piran[11] identify the dynamical variable η somewhat differently than was done in (19b),

$$\eta=B^2-1. \tag{21}$$

As in QI gauge, the variables η and ξ are evolved, while A is derived from the (now parabolic) Hamiltonian constraint.

The weak-field exterior solution given in Sec. II can now be transformed to QI and RD gauges. We must find the infinitesimal gauge transformations from the LT gauge using

$$h_{\alpha\beta}=h^{(nr)}_{\alpha\beta}+\nabla_\alpha\zeta_\beta+\nabla_\beta\zeta_\alpha, \tag{22}$$

that take us to the relevant numerical relativity gauge indicated by (nr). The spatial generators can be quite generally written in terms of (pure-orbit) vector spherical harmonics:

$$\zeta_i = \sum_{l',l,m} \Phi_{l'l} \tilde{Y}_i^{l',lm}, \tag{23}$$

where the scaled vector harmonics $\tilde{\mathbf{Y}}^{l',lm}$ (with tilde) are defined by (A23). LT gauge is a special form in which not all tensor harmonics appear at a given order l. In a typical gauge, however, the metric may involve a superposition of all harmonics:

$$h_{ij} = \sum_{\lambda,l',l} A_{\lambda l',l} \tilde{T}_{ij}^{\lambda\, l',lm}, \tag{24}$$

where the scaled tensor harmonics are defined by (A24). The scalings on the vector and tensor harmonics are introduced so that components maintain simple forms in terms of the amplitudes $\Phi_{l'l}$ and $A_{\lambda l',l}$ and trigonometric functions.

We do not consider time-slicing conditions in this paper and therefore do not obtain the time component of the generator. Hence, computation of the source's total angular momentum (which requires the time-slicing influenced shift vector components $\beta_j = g_{0j}$) will be considered elsewhere. The spatial part of transformation (22) involves the Killing operator

$$(K\zeta)_{ij} = \nabla_i \zeta_j + \nabla_j \zeta_i. \tag{25}$$

In the Appendix we give the decomposition of (25) in terms of the scaled harmonics mentioned above.

In order to transform the solution (16), we need to retain all terms in (23) through $l=3$ subject to the constraints of axisymmetry $(m=0)$ and equatorial plane symmetry:

$$\zeta_i = \Phi_{10}\tilde{Y}_i^{1,00} + \Phi_{12}\tilde{Y}_i^{1,20} + \Phi_{32}\tilde{Y}_i^{3,20} + \Phi_{11}\tilde{Y}_i^{1,10} + \Phi_{33}\tilde{Y}_i^{3,30}. \tag{26}$$

Using (A25), one arrives, after some manipulation, at

$$(K\zeta)_{rr} = -2\,\partial_r\Phi_{10} + 2\,P_2\,\partial_r(\Phi_{12}-\Phi_{32}), \tag{27a}$$

$$(K\zeta)_{\theta\theta} = \frac{1}{r}(\Phi_{12} - 2\Phi_{10} + \tfrac{2}{3}\Phi_{32}) - \frac{2}{3r}P_2(3\Phi_{12}+7\Phi_{32}), \tag{27b}$$

$$(K\zeta)_{\phi\phi} = -\frac{1}{r}(\Phi_{12}+2\Phi_{10}+\tfrac{2}{3}\Phi_{32}) - \frac{10}{3r}P_2\,\Phi_{32}, \tag{27c}$$

$$(K\zeta)_{r\theta} = -(\tfrac{3}{2}D_0^-\Phi_{12} + D_4^+\Phi_{32})\sin\theta\cos\theta, \tag{27d}$$

$$(K\zeta)_{r\phi} = -D_1^+\Phi_{11}\sin\theta - \tfrac{3}{2}D_1^+\Phi_{33}\sin\theta\,(5\cos^2\theta - 1), \tag{27e}$$

$$(K\zeta)_{\theta\phi} = \frac{15}{r}\Phi_{33}\sin^2\theta\cos\theta, \tag{27f}$$

where the raising and lowering operators D^+ and D^- are defined in the Appendix.

QI and RD gauges have two conditions in common, (18b) and (18c), which in the weak-field limit become

$$h_{r\phi}^{(nr)} = 0, \qquad h_{r\theta}^{(nr)} = 0. \tag{28}$$

Equations (28) lead to the following conditions on several of the $\Phi_{l'l}$:

$$D_1^+\Phi_{11} = 0, \tag{29}$$

$$D_1^+\Phi_{33} = \tfrac{2}{15}\{S^{(3)}\}_2, \tag{30}$$

$$\tfrac{3}{2}D_0^-\Phi_{12} + D_4^+\Phi_{32} = 2\{I^{(2)}\}_0\,. \tag{31}$$

A. Quasi-isotropic gauge

We now complete the transformation to QI gauge. Linearization of the natural variables defined in (18a), (19a), and (19b) leads to

$$\eta = \tfrac{1}{2}(h_{\theta\theta}^{\rm QI} - h_{\phi\phi}^{\rm QI}), \tag{32a}$$

$$\phi = 1 + \tfrac{1}{6}(h_{\theta\theta}^{\rm QI} + \tfrac{1}{2}h_{\phi\phi}^{\rm QI}), \tag{32b}$$

$$\xi = h_{\theta\phi}^{\rm QI}. \tag{32c}$$

In the weak-field limit, the QI gauge condition (18d) reduces to the form

$$h_{rr}^{\rm QI} - h_{\theta\theta}^{\rm QI} = 0. \tag{33}$$

Equation (33), along with (27a) and (27b), then leads to the following two conditions:

$$2D_1^+\Phi_{10} + \frac{1}{r}\Phi_{12} + \frac{2}{3r}\Phi_{32} = \tfrac{2}{3}\{I^{(2)}\}_0, \tag{34}$$

$$3D_0^-\Phi_{12} - \left[3\partial_r - \frac{7}{r}\right]\Phi_{32} = 4\{I^{(2)}\}_0. \tag{35}$$

Simultaneously solving (29), (30), (31), (34), and (35), we find, after neglecting several radially divergent homogeneous terms, that

$$\Phi_{11} = \Phi_{32} = 0, \tag{36a}$$

$$\Phi_{10} = \tfrac{1}{4}\Phi_{12} = -\tfrac{1}{3}\epsilon\frac{I^{(1)}}{r} - \tfrac{1}{6}\epsilon\frac{b_2(t)}{r}, \tag{36b}$$

$$\Phi_{33} = -\tfrac{2}{15}\epsilon\{S^{(2)}\}_1 - \tfrac{1}{15}c_3(t)r, \tag{36c}$$

where $b_2(t)$ and $c_3(t)$, which result as homogeneous solutions to the differential equations for the $\Phi_{l'l}$, are time-dependent pure-gauge functions. Although the pure-gauge term involving $c_3(t)$ is radially divergent, we retain it and discuss its significance in the next section.

Now that we have the generating vector field of the gauge transformation, the changes (27) in the metric components become

$$(K\zeta)_{rr}=\frac{1}{3}\left[2\{I^{(2)}\}_1+\epsilon\frac{b_2}{r^2}\right](4P_2-1), \tag{37a}$$

$$(K\zeta)_{\theta\theta}=\frac{1}{3}\left[2\epsilon\frac{I^{(1)}}{r^2}+\epsilon\frac{b_2}{r^2}\right](4P_2-1), \tag{37b}$$

$$(K\zeta)_{\phi\phi}=2\epsilon\frac{I^{(1)}}{r^2}+\epsilon\frac{b_2}{r^2}, \tag{37c}$$

$$(K\zeta)_{r\theta}=-2\{I^{(2)}\}_0\sin\theta\cos\theta, \tag{37d}$$

$$(K\zeta)_{r\phi}=-\tfrac{1}{5}\{S^{(3)}\}_2\sin\theta\,(5\cos^2\theta-1), \tag{37e}$$

$$(K\zeta)_{\theta\phi}=\left[-2\epsilon\frac{S^{(2)}}{r^2}-2\frac{S^{(1)}}{r^3}-c_3\right]\sin^2\theta\cos\theta. \tag{37f}$$

Employing Eq. (22), we apply (37) and transform the metric (16), which yields the following set of pure-orbit terms, as in (24), for the metric in QI gauge through $l=3$:

$$\begin{aligned}h_{ij}^{\rm QI}=&A_{00,0}\tilde{T}_{ij}^{0\,0,00}+A_{02,2}\tilde{T}_{ij}^{0\,2,20}+A_{20,2}\tilde{T}_{ij}^{2\,0,20}\\&+A_{22,0}\tilde{T}_{ij}^{2\,2,00}+A_{22,2}\tilde{T}_{ij}^{2\,2,20}\\&+A_{22,3}\tilde{T}_{ij}^{2\,2,30}+A_{24,3}\tilde{T}_{ij}^{2\,4,30},\end{aligned} \tag{38}$$

with amplitudes given as

$$A_{00,0}=\frac{2M}{r}+\frac{1}{9}\left[2\frac{I^{(2)}}{r}-2\epsilon\frac{I^{(1)}}{r^2}-\epsilon\frac{b_2}{r^2}\right], \tag{39a}$$

$$A_{02,2}=-\frac{2}{9}\left[\frac{I^{(2)}}{r}-\epsilon\frac{I^{(1)}}{r^2}-9\frac{I}{r^3}+4\epsilon\frac{b_2}{r^2}\right], \tag{39b}$$

$$A_{20,2}=\frac{4}{9}\left[\frac{I^{(2)}}{r}+2\epsilon\frac{I^{(1)}}{r^2}+\epsilon\frac{b_2}{r^2}\right], \tag{39c}$$

$$A_{22,0}=A_{20,2}=-\tfrac{1}{2}A_{22,2}, \tag{39d}$$

$$A_{24,2}=0, \tag{39e}$$

$$\begin{aligned}A_{22,3}&=-A_{24,3}\\&=-\frac{4}{21}\left[\frac{S^{(3)}}{r}+5\epsilon\frac{S^{(2)}}{r^2}+5\frac{S^{(1)}}{r^3}+c_3\right],\end{aligned} \tag{39f}$$

$$A_{22,1}=0. \tag{39g}$$

Using Eqs. (38) and (39) for the QI metric perturbation and the definitions (32) for the (linearized) natural variables, we find

$$\eta=\sin^2\theta\left[\frac{I^{(2)}}{r}+2\epsilon\frac{I^{(1)}}{r^2}+\epsilon\frac{b_2}{r^2}\right], \tag{40a}$$

$$\begin{aligned}\phi=&1+\frac{M}{2r}-\epsilon\frac{b_2}{4r^2}+\frac{I}{2r^3}\\&+\sin^2\theta\left[\frac{1}{12}\frac{I^{(2)}}{r}-\tfrac{1}{12}\epsilon\frac{I^{(1)}}{r^2}-\frac{3}{4}\frac{I}{r^3}+\epsilon\frac{b_2}{3r^2}\right],\end{aligned} \tag{40b}$$

$$\xi=\sin^2\theta\cos\theta\left[\frac{S^{(3)}}{r}+5\epsilon\frac{S^{(2)}}{r^2}+5\frac{S^{(1)}}{r^3}+c_3\right], \tag{40c}$$

for the asymptotic structure of the three-metric variables in QI gauge. Compare η (40a) in this gauge with its forms in LT gauge (17a), TT gauge (17b), and (jumping ahead) RD gauge (49a) and note how the near-zone field is altered and the gauge terms are introduced. The gauge term $b_2(t)$ appearing in the quadrupole part of the expansion[4,26,28] falls off as r^{-2} in QI gauge.

B. Radial gauge

We can now proceed in similar fashion to find the transformation of the LT gauge solution (16) into RD gauge. In the weak-field limit, the RD gauge metric variables become

$$\eta=\tfrac{1}{2}(h_{\phi\phi}-h_{\theta\theta}), \tag{41a}$$

$$A=1+\tfrac{1}{2}h_{rr}, \tag{41b}$$

$$\xi=h_{\theta\phi}. \tag{41c}$$

Note that Bardeen and Piran[11] define η with a sign difference compared to Eqs. (17a) and (32a). The uniquely defining condition for RD gauge (20b) becomes, when linearized,

$$h_{\theta\theta}^{\rm RD}+h_{\phi\phi}^{\rm RD}=0. \tag{42}$$

Equation (42) leads to conditions on the generator functions (26):

$$\Phi_{10}=-M, \tag{43}$$

$$\tfrac{1}{2}\Phi_{12}+2\Phi_{32}=-\epsilon\{I^{(1)}\}_1. \tag{44}$$

By solving (44) simultaneously with (29), (30), and (31), we arrive at

$$\begin{aligned}\Phi_{12}=&-\frac{6}{5}\left[\epsilon\frac{I^{(1)}}{r}-\frac{I}{r^2}+\frac{2}{r^2}\int_0^r\frac{I(t-\epsilon r')}{r'}dr'\right.\\&\left.+\frac{2}{3}\frac{b_2'(t)}{r^2}\right],\end{aligned} \tag{45a}$$

$$\begin{aligned}\Phi_{32}=&-\frac{1}{5}\left[\epsilon\frac{I^{(1)}}{r}+4\frac{I}{r^2}-\frac{3}{r^2}\int_0^r\frac{I(t-\epsilon r')}{r'}dr'\right.\\&\left.-\frac{b_2'(t)}{r^2}\right],\end{aligned} \tag{45b}$$

while the current octupole parts are identical to those in QI gauge: Eqs. (36a) and (36c). The integral terms that appear in (45a) and (45b) are related to the outward parabolic integration that defines the shift vector in RD gauge.[11] In the linearized case, the integrations are formal only and cannot be extended into the strong-field region. Hence the integrals in (45a) and (45b) will be unknown and can be subsumed into the homogeneous solution term $b_2'(t)/r^2$ (Ref. 29):

$$b_2(r,t)\equiv b_2'(t)+3\int_0^r\frac{I(t-\epsilon r')}{r'}dr', \tag{46}$$

though now, in contrast to the QI gauge case, this gauge term is a function of radius as well as time. The generating vector field is now used to produce the metric in RD gauge. Analogous to (38) we expand the RD metric in terms of pure-orbit harmonics through $l=3$:

$$h_{ij}^{\mathrm{RD}} = A_{00,0}\tilde{T}_{ij}^{0\,0,00} + A_{02,2}\tilde{T}_{ij}^{0\,2,20} + A_{20,2}\tilde{T}_{ij}^{2\,0,20} + A_{22,0}\tilde{T}_{ij}^{2\,2,00} + A_{22,2}\tilde{T}_{ij}^{2\,2,20} + A_{24,2}\tilde{T}_{ij}^{2\,4,20} + A_{22,3}\tilde{T}_{ij}^{2\,2,30} + A_{24,3}\tilde{T}_{ij}^{2\,4,30}, \quad (47)$$

with amplitudes given as

$$A_{00,0} = \tfrac{1}{2}A_{22,0} = \frac{2M}{3r}, \quad (48a)$$

$$A_{02,2} = \frac{4}{3}\left[\epsilon\frac{I^{(1)}}{r^2} + 4\frac{I}{r^3} - \frac{b_2}{r^3}\right], \quad (48b)$$

$$A_{20,2} = \tfrac{8}{15}\{I^{(2)}\}_2, \quad (48c)$$

$$A_{22,2} = -\tfrac{10}{7}A_{20,2} + \tfrac{8}{7}A_{02,2}, \quad (48d)$$

$$A_{24,2} = \tfrac{3}{7}A_{20,2} + \tfrac{6}{7}A_{02,2}, \quad (48e)$$

while the current octupole amplitudes are identical to those in QI gauge and are already given by (39f) and (39g). The three spatial metric variables in RD gauge then have the asymptotic forms

$$\eta = -\sin^2\theta\left[\frac{I^{(2)}}{r} + 2\epsilon\frac{I^{(1)}}{r^2} - \frac{I}{r^3} + \frac{b_2}{r^3}\right], \quad (49a)$$

$$A = 1 + \frac{M}{r} + P_2\left[2\epsilon\frac{I^{(1)}}{r^2} + 8\frac{I}{r^3} - 2\frac{b_2}{r^3}\right], \quad (49b)$$

$$\xi = \sin^2\theta\cos\theta\left[\frac{S^{(3)}}{r} + 5\epsilon\frac{S^{(2)}}{r^2} + 5\frac{S^{(1)}}{r^3} + c_3\right]. \quad (49c)$$

As pointed out by Bardeen and Piran,[11] the mass quadrupole gauge term in RD gauge formally falls like r^{-3}, one power faster than its analogue in QI gauge. The current octupole moment appears in the variable ξ with the same form as it has in QI gauge (40c).

C. Discussion

Equations (39) and (40) for QI gauge and (48) and (49) for RD gauge represent our matching templates. It can be seen that the practical effect of identifying "dynamical" metric variables [such as the two definitions of η in (19b) and (21)] was to eliminate the appearance of the mass monopole term. However, as is evident in (40a) and (49a) as well as expressions (40c) and (49c) for ξ, the asymptotic structure of these variables at any finite radius contains, in addition to the radiation terms $I^{(2)}(t-\epsilon r)/r$ and $S^{(3)}(t-\epsilon r)/r$, the near-zone field [terms with lower derivatives of $I(t-\epsilon r)$ and $S(t-\epsilon r)$] and gauge terms b_2 and c_3. It has been stated[9] that the current moment part ξ of the linear solution is gauge invariant. This is true of the leading (waveform) part of the solution [as in our Eq. (12)], but, as we see from comparing (16j) with (40c) and (49c), the near-zone field is altered by the transformation, and a gauge term is introduced. It is impossible to determine simply from the different formal rates of fall off of the mass quadrupole gauge terms b_2 which gauge provides the minimum distortion in the radiative variable η at any given radius. The matching given in the next section sidesteps these gauge effects to get directly to the asymptotic waveforms.

IV. READING OFF GRAVITATIONAL WAVES

By numerically sampling all of the multipole moment amplitudes we obtain sufficient information to solve for the component parts of the matching templates for QI and RD gauges. The amplitudes can be computed via surface integrals using (A5) and (A24):

$$A_{\lambda l',l} = (d_{\lambda l',l})^{-1}\int d\Omega\, h_{ij}T_{ij}^{\lambda\, l',l0}. \quad (50)$$

We now separately detail the matchings for the two gauges.

A. Matching to quasi-isotropic gauge

Expression (50) for the amplitudes $A_{\lambda l',l}$ can be evaluated for the QI metric in terms of the natural variables (19):

$$A_{00,0} = \int_0^{\pi/2} d\theta\, \sin\theta\, (\phi^4 - 1), \quad (51a)$$

$$A_{02,2} = 5\int_0^{\pi/2} d\theta\, \sin\theta\, P_2\, (\phi^4 - 1), \quad (51b)$$

$$A_{20,2} = \tfrac{2}{3}\int_0^{\pi/2} d\theta\, \sin\theta\, \eta, \quad (51c)$$

$$A_{22,3} = \tfrac{5}{2}\int_0^{\pi/2} d\theta\, \sin^3\theta\, \cos\theta\, \xi, \quad (51d)$$

$$A_{20,2} + \tfrac{1}{2}A_{22,2} = \tfrac{2}{7}\int_0^{\pi/2} d\theta\, \sin\theta\, (5\cos^2\theta - 1)\, \eta = A_{24,2} = 0. \quad (51e)$$

These amplitudes can easily be obtained as numerical time series at a set of extraction radii during a simulation. Note that the last equation (51e) can be used as a consistency check and a measure of the accuracy to which a given level of numerical resolution in the angular direction maintains orthonormality of the Legendre polynomials.[30]

Assume for now that there is one extraction radius $r=r_0$. By combining (39b) and (39c) and evaluating at r_0, we get an equation for just the quadrupole moment $I(t-r_0)$,

$$I^{(2)}(t-r_0) + \frac{3}{r_0}I^{(1)}(t-r_0) + \frac{3}{r_0^2}I(t-r_0) = 3r_0(A_{20,2} + \tfrac{1}{2}A_{02,2}) \equiv Q(t;r_0), \quad (52)$$

separated from other effects [i.e., the combination of amplitudes yielding $Q(t;r_0)$ is free of pure-gauge terms]. We have set $\epsilon=+1$ for outgoing radiation since such a boundary condition will be imposed on the outer boundary. At a fixed radius r_0, Eq. (52) can be interpreted as

an ordinary differential equation (ODE) in time for the quadrupole moment. If this ODE is solved for $I(t-r_0)$, $I^{(1)}(t-r_0)$, and $I^{(2)}(t-r_0)$ (we discuss this below), then using (39c) we obtain the mass quadrupole gauge function

$$b_2(t)=\tfrac{9}{4}r_0{}^2A_{20,2}-r_0\,I^{(2)}(t-r_0)-2I^{(1)}(t-r_0). \tag{53}$$

In the weak-field region, b_2 should be independent of radius, and so by using a set of extraction two-surfaces with different radii we obtain an important check on the reliability of the matching. Combining (53) with (39a) we find the mass monopole moment

$$M=\tfrac{1}{8}r_0(4A_{00,0}+A_{20,2})-\tfrac{1}{6}I^{(2)}(t-r_0). \tag{54}$$

This is a quasilocal mass indicator with first-order corrections for the effects of the global gauge shear and the shearing effects of the gravitational waves crossing the extraction two-surface.[31] Subject to solving (52), this completes the matching for the mass moments $l=0$ and $l=2$.

Before considering the $l=3$ current octupole, we discuss the solution of the ODE (52). At a finite radius one cannot instantaneously determine the radiation field. But by integrating (52) over the past timelike cylinder swept out by the extraction two-surface, we can determine the quadrupole moment $I(t-r_0)$ and from it its first two derivatives, subject to the initial values $I_0=I(t_0-r_0)$ and $\dot{I}_0=I^{(1)}(t_0-r_0)$. To get a better understanding of how the radiation is being separated from the near-zone field it is useful to consider the general solution of (52) constructed via the Laplace transform [we do not suggest the use of this expression numerically; it is better to split (52) into first-order form in time and to integrate with the simulation time step]:

$$\begin{aligned}I(t-r_0)=&\frac{1}{\omega}\int_0^t Q(t';r_0)\,e^{-\gamma(t-t')}\sin\omega(t-t')\,dt'\\&+I_0\,e^{-\gamma t}\cos\omega t\\&+\frac{1}{\omega}\left[\dot{I}_0+\frac{1}{\tau}I_0\right]e^{-\gamma t}\sin\omega t,\end{aligned} \tag{55}$$

where we have taken the initial slice to coincide with $t=0$. We find a damping time τ and frequency ω for the *transients*

$$\tau=\frac{1}{\gamma}=\tfrac{2}{3}r_0,\qquad \omega=(\tfrac{3}{4})^{1/2}r_0^{-1}, \tag{56}$$

defined at the chosen extraction radius. We see that, with the choice $\epsilon=+1$ (outgoing waves) made in writing (52), the Green's function has a decaying exponential behavior. Correspondingly, the influence of the initial values I_0 and $\dot{I}_0$ dies out in a time of order the light travel time across the extraction radius. Thus, errors in determining the initial values will act as transients. In collapse problems the free fall time scale $t_{\rm ff}$ from r_0 is related to the light crossing time $t_0=r_0$ by $t_{\rm ff}\approx t_0(r_0/M)^{1/2}$. Thus, $t_{\rm ff}$ is at least several e-folding times so the initial values for the integration can be largely ignored. Nonetheless, we will describe in a subsequent paper the evaluation of the initial values for the moments.

We have made two immediate tests of these ideas. We first performed a simple test of the separation of radiation from near-zone field by calculating numerical evolutions of the (1D) radial wave equation (A6) for $l=2$. This equation was split into first-order form and integrated with a fully second-order accurate finite difference scheme.[12] An outgoing radiation boundary condition was applied at the outer boundary, and the inner zones were forced to oscillate to produce outgoing radiation with a prescribed waveform. The outer boundary sat well out in the wave zone, while we evaluated (52) at several radii near or within the transition region with the approximate locations $\lambda\!\!\!^{-}/r=$ 4.0, 2.0, 1.0, 0.5, 0.25. The amplitude $r\phi$ sampled at large values of $\lambda\!\!\!^{-}/r$ (deep in the near zone) differed significantly from the asymptotic (constant) amplitude of $r\phi$, closely following the expected scaling $[1+3(\lambda\!\!\!^{-}/r)^2+9(\lambda\!\!\!^{-}/r)^4]^{1/2}$, yet the integration of (52) using the simulation time step, followed by differentiation to obtain $rI^{(2)}$, picks off the asymptotic value quite accurately at all our chosen values of $\lambda\!\!\!^{-}/r$.

The second test involved numerical modeling with a full 2D general relativistic finite difference code the quadrupole small amplitude oscillations of relativistic neutron-star models.[4] Equilibrium relativistic stars constructed from tabulated or polytropic equations of state were modeled on a spherical-polar mesh. The equilibrium fluid configuration was slightly deformed by a quadrupole displacement vector. The Hamiltonian constraint was then solved to provide consistent initial data and the configuration was time evolved. The oscillations of the star immediately drive a radiation front out into the vacuum region surrounding the star. Once the front has left the edge of the mesh (where an outgoing radiation boundary condition is employed), a steady quadrupole radiation field sets up outside the star.

In a first test of the extraction technique, we examined the ability to read off the pure-gauge coefficient $b_2(t)$. Taking the extraction two-surface to lie fairly deep in the local wave zone, $Q(t;r_0)$ in (52) directly gave a measure of $I^{(2)}(t-r_0)$. Then using this in (53), and again ignoring the smaller (in this case) $I^{(1)}(t-r_0)$ term, we obtained values of b_2 as a function of time. The contribution of the pure-gauge piece can then be seen by comparing in Fig. 1 the "raw" waveform $\eta/\sin^2\theta$ [cf. Eq. (40a)] with the gauge-corrected waveform $\eta/\sin^2\theta-b_2(t)/r^2$. The "wave" present early on is entirely due to the gauge effect.

We now turn our attention to the current octupole wave. By examining (39f) and (39g), it is clear that there is no way to algebraically eliminate the appearance of the pure-gauge term $c_3(t)$. This term arises as a slight irregularity in the metric due to the gauge choice (18b). There are two ways of proceeding. As Bardeen and Piran[11] have pointed out, this term arises from the parabolic radial integration for the azimuthal component of the shift vector β^ϕ. The radial integration can be performed either outward or inward. Bardeen and Piran

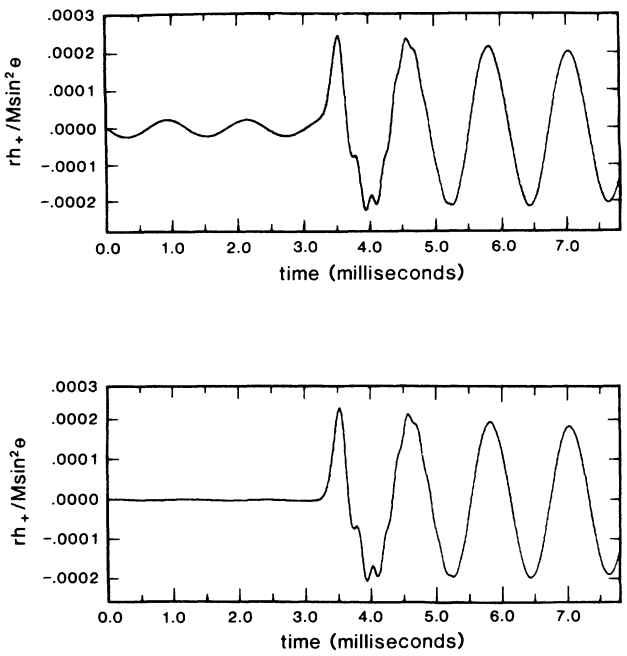

FIG. 1. Waveforms from a finite amplitude quadrupole oscillation of a relativistic neutron-star model. Times series are obtained near the outer boundary of the finite difference mesh. The upper plot displays the "raw" waveform found from sampling $r\eta$ along the equatorial plane $\theta=\pi/2$. The lower plot shows the "corrected" waveform that results after subtracting the effects of the mass quadrupole pure-gauge term which arises in quasi-isotropic gauge. It is now more clearly evident that the pulsation drives a sharp wave front outward from the star, which abruptly reaches the extraction radius at 3.25 ms. The oscillation seen in the first plot prior to this time is purely an instantaneous (elliptic) gauge effect. The radiation field shown in the second plot settles into a 1.2-ms period sine wave within several oscillations.

opt for outward integration, which allows β^{ϕ} and ξ to be regular at $r=0$ but irregular as $r\to\infty$ [the $c_3(t)$ term]. If instead the integration were taken inward, demanding regularity as $r\to\infty$ would imply choosing $c_3(t)=0$ and the irregularity would show up at $r=0$ instead.

If inward integration is adopted, Eq. (39f) with $c_3(t)=0$ could then be directly integrated on the extraction two-surface to yield $S^{(1)}(t-r_0)$ and, in turn, the current octupole asymptotic waveform $S^{(3)}(t-r)/r$. Nevertheless, the waveform can also be obtained if outward integration is adopted by slightly modifying our procedure. As Bardeen and Piran[11] point out, ξ can be replaced by $\partial_r\xi$ as the radiative variable. We can then modify the two-surface extraction integration (51d) to provide an amplitude:

$$A'_{22,3}=\frac{5}{2}\int_0^{\pi/2}d\theta\,\sin^3\theta\,\cos\theta\,\partial_r\xi. \tag{57}$$

By referring to Eq. (40c), we see that the asymptotic structure of $\partial_r\xi$ is

$$\partial_r\xi=-\epsilon\,\sin^2\theta\,\cos\theta\{S^{(4)}\}_3, \tag{58}$$

and $c_3(t)$ does not enter. Interestingly, unlike the radial part of (40c), the radial terms in (58) are precisely a solution (A13) to the radial wave equation. This point will be discussed in more detail in later work. Using (58) we then have the ODE

$$\frac{S^{(4)}}{r}+6\frac{S^{(3)}}{r^2}+15\frac{S^{(2)}}{r^3}+15\frac{S^{(1)}}{r^4}=\tfrac{21}{4}A'_{22,3} \tag{59}$$

from which to determine the current octupole waveform.

B. Matching to radial gauge

The RD gauge amplitudes are evaluated via surface integrals in terms of the natural variables, (20a) and (21), identified by Bardeen and Piran[11]

$$A_{00,0}=\tfrac{2}{3}\int_0^{\pi/2}d\theta\,\sin\theta\,(A-1), \tag{60a}$$

$$A_{02,2}=\tfrac{10}{3}\int_0^{\pi/2}d\theta\,\sin\theta\,P_2\,(A-1), \tag{60b}$$

$$A_{20,2}=\tfrac{4}{3}\int_0^{\pi/2}d\theta\,\sin\theta[P_2\,(A-1)-\tfrac{3}{4}\sin^2\theta\,\eta], \tag{60c}$$

As described for QI gauge, these amplitudes are obtained as numerical time series at a set of extraction radii during a simulation.

In direct analogy with (52), Eq. (48c) yields an ODE for the quadrupole moment:

$$I^{(2)}(t-r_0)+\frac{3}{r_0}I^{(1)}(t-r_0)+\frac{3}{r_0^2}I(t-r_0)=\tfrac{15}{8}r_0A_{20,2}, \tag{61}$$

which when integrated allows the radiation amplitude to be separated from the near-zone field. The mass is also trivial to obtain using (48a):

$$M=\tfrac{3}{2}r_0A_{00,0}. \tag{62}$$

As noted in Sec. III B, the current octupole moment appears in the RD gauge metric perturbation with the same form as it does in QI gauge. Thus, the waveform extraction for RD gauge is identical to that given in Eqs. (57)–(59).

V. READING OFF WAVEFORMS USING THE RIEMANN TENSOR

Smarr[32] has described a waveform extraction technique which relied on the calculation of components of the Riemann tensor. By using the TT gauge result

$$\ddot{h}_{ij}^{\rm TT}=-2R_{titj}, \tag{63}$$

the two polarization states were to be determined by performing a double time integration of (63):

$$h_+^{\rm TT}=\eta=\tfrac{1}{2}(h_{\theta\theta}^{\rm TT}-h_{\phi\phi}^{\rm TT})=2\int_{t_0}^{t}dt'\int_{t_0}^{t'}dt''\,(R_{t\phi t\phi}-R_{t\theta t\theta}), \tag{64}$$

$$h_\times^{\rm TT}=\xi=h_{\theta\phi}^{\rm TT}=-2\int_{t_0}^{t}dt'\int_{t_0}^{t'}dt''\,R_{t\theta t\phi}. \tag{65}$$

The reasoning behind this suggestion was to use the invariance of the Riemann tensor under gauge changes in the weak-field limit to allow an unambiguous evaluation of h_+^{TT} and $h_\times^{TT}$ in any numerically useful gauge. The problem that arises in this scheme is that the integration for h_+^{TT} or $h_\times^{TT}$ is unique only up to terms such as $a_0+a_1(t-r)$, where a_0 and a_1 are constants which naturally arise in integrating (63). These give a misleading appearance to the waveform. As Teukolsky has discussed (in Sec. III of Ref. 15), these are pure-gauge terms. We can see this more clearly if we just focus on the mass quadrupole moment contribution to (64). We know from (14) that the mass quadrupole part of the gravitational field is uniquely determined by the moment $I(t-r)$ (and its derivatives). Yet, if we examine the form of η (or h_+^{TT}) in TT gauge (17b), we see that it depends on $I^{(-1)}(t-r)$ and $I^{(-2)}(t-r)$ as well. These integrals of I involve arbitrary integration constants that give $I^{(-2)}$, and hence η, an additional dependence like $I^{(-2)}=a_0+a_1(t-r)$. Thus residual arbitrariness exists in h_+^{TT}. Based on this and the discussion in Sec. IV A, we see it is the moment $I(t-r)$ and its derivative $I^{(2)}(t-r)$ that should be calculated to give the asymptotic radiation.

Utilizing the matching ideas in Sec. IV it is possible to find an attractive modification of this scheme that preserves the use of the gauge invariance of the Riemann tensor. To do this, we reexpress Teukolsky's TT solution in our notation[15]

$$h_{ij}^{TT}=\tfrac{8}{15}\{I^{(2)}\}_0\,\tilde{T}_{ij}^{2\,0,20}-\tfrac{16}{21}\{I^{(2)}\}_2\,\tilde{T}_{ij}^{2\,2,20}+\tfrac{8}{35}\{I^{(2)}\}_4\,\tilde{T}_{ij}^{2\,4,20}. \tag{66}$$

Taking two time derivatives and integrating over the two-surface we find

$$\{I^{(4)}\}_4=\tfrac{35}{8}(d_{24,2})^{-1}\int d\Omega\,\ddot{h}_{ij}^{TT}\,T_{ij}^{2\,4,20}, \tag{67a}$$

$$\{I^{(4)}\}_2=-\tfrac{21}{16}(d_{22,2})^{-1}\int d\Omega\,\ddot{h}_{ij}^{TT}\,T_{ij}^{2\,2,20}, \tag{67b}$$

and

$$\{I^{(4)}\}_0=\tfrac{15}{8}(d_{20,2})^{-1}\int d\Omega\,\ddot{h}_{ij}^{TT}\,T_{ij}^{2\,0,20} \tag{67c}$$

for the radial wave solutions.

By directly using (67b) and substituting (63) to put the result in terms of the Riemann tensor, we obtain an equation which can be integrated for the second time derivative of I,

$$I^{(4)}(t-r_0)+\frac{3}{r_0}I^{(3)}(t-r_0)+\frac{3}{r_0^2}I^{(2)}(t-r_0)=\tfrac{5}{4}r_0\int d\theta\,\sin\theta[P_2\,R_{trtr}-\tfrac{1}{2}R_{t\theta t\theta}-(\tfrac{3}{2}\cos\theta-1)\,R_{t\phi t\phi}-\tfrac{3}{2}\sin\theta\cos\theta\,R_{tr t\theta}], \tag{68}$$

in a manner analogous to equations we have already discussed in Sec. IV A. Here however, because (68) depends on computing the Riemann tensor, the result is gauge invariant (to linear order). Hence this formula should be useful in numerical calculations irrespective of the gauge employed. As we see from (55), the integration constants, which we should be able to determine from initial data, interestingly contribute effects to the waveform which exponentially decay away, in contrast with the integration constants of (63).

VI. DISCUSSION

We have shown that the direct use of *radiative* metric variables at a finite radius to determine emitted gravitational waveforms in numerical relativity calculations is biased by both time-dependent gauge and near-zone effects. In certain calculations these effects may be virtually negligible; in other calculations these effects will have to be determined and removed to properly extract the asymptotic waveforms. Even in circumstances where gauge and near-zone effects are expected to be negligible it is important (and relatively simple) to demonstrate the fact.

Stark and Piran[33] have analyzed the sensitivity of waveforms sampled directly from the radiative variable in RD gauge to changes in the observation radius. Their waveforms resulted from the collapse of a rotating relativistic polytrope to form a black hole. They report relatively reproducible waveforms (particularly in the late time ring-down phase) for five different observation radii. In terms of the late time wavelength ($\lambda\sim 20M$) these radii range from $\sim 2.5\lambda$ to $\sim 0.7\lambda$. The critical number which determines the importance of near-zone effects is the ratio of the reduced wavelength to observation radius, $\lambda\!\!\!^{-}/r$. Even the smallest observation radius of Stark and Piran, $r\sim 4.4\lambda\!\!\!^{-}$, is still fairly far out into the *local wave zone.* At this distance, the near-zone effects on the waveform amplitude were only $\sim 9\%$. It would be useful to also have an analysis of the size of the gauge effect in the Stark-Piran calculations. The gauge effect may be responsible for the larger discrepancies between their sampled waveforms evident at earlier times, prior to the ring-down phase.

The collapse of a star to a black hole is an extreme case, producing the smallest possible dimensionless wavelength ($\lambda\!\!\!^{-}/M\sim 2.8$). Other collapse scenarios in which an object hydrodynamically turns around, or *bounces,* will emit radiation with dimensionless wavelengths that typically are much larger: roughly

$$\frac{\lambda\!\!\!^{-}}{M}\sim\left[\frac{R}{M}\right]^{3/2}, \tag{69}$$

where R is the characteristic radius of the object at bounce. For a collapsing stellar core reaching its first bounce, this radius might be $R \sim 15M$, giving a reduced dimensionless wavelength of $\lambda\!\!\!^{-} \sim 60M$. To evaluate the waveforms in this case, without accounting for gauge and near-zone effects, the observation radius may need to exceed $300M$.

In a subsequent paper we will subject these radiation extraction methods to a set of numerical tests. We will also detail another method for reading off gravitational waves which, like the Riemann-tensor-based method, should be applicable in arbitrary spatial gauges. These methods will have to be carefully tested to judge which is most suitable for numerical use. Since the method given in this paper in Sec. III, using a matching template, allows one to obtain a complete breakdown of the metric variables, it should be simple to use the matching to further improve the outgoing radiation boundary condition to take into account the gauge and near-zone field effects.

ACKNOWLEDGMENTS

We gratefully acknowledge helpful discussions with S. Finn, D. Hobill, R. Isaacson, B. Schutz, L. Smarr, and K. Thorne. We thank K. Thorne, S. Finn, and D. Hobill for careful readings of the manuscript. This research was supported in part by NSF Grants Nos. PHY83-08826 and AST85-14911. Calculations were performed at the NSF National Center for Supercomputing Applications at the University of Illinois.

APPENDIX

In expressing the general weak-field solution in Sec. II and subsequent transformations from it, we use pure-orbit vector spherical harmonics $\mathbf{Y}^{l',lm}$ and pure-orbit tensor spherical harmonics $\mathbf{T}^{\lambda\, l',lm}$. The properties of these harmonics are summarized in Thorne[3] and further material can be found in Edmonds,[34] Mathews,[35] and Zerilli.[36] Components can be derived using the formulas found in Edmonds or looked up in Mathews. The order of the representation group is λ, while l', l, and m are, respectively, the orbital, total, and azimuthal angular momentum quantum numbers. The vector and tensor pure-orbit harmonics are eigenfunctions of the orbital angular momentum operator

$$\mathbf{L}^2 = -r^2\nabla^2 + \partial_r r^2 \partial_r . \tag{A1}$$

Hence,

$$\mathbf{L}^2\ \mathbf{Y}^{l',lm} = l'(l'+1)\mathbf{Y}^{l',lm}, \tag{A2}$$

$$\mathbf{L}^2\ \mathbf{T}^{\lambda\, l',lm} = l'(l'+1)\mathbf{T}^{\lambda\, l',lm}. \tag{A3}$$

Like the scalar spherical harmonics Y^{lm}, they satisfy orthonormality relations:

$$\int Y_j^{L,lm}\ Y_j^{L',l'm'*} d\Omega = \delta_{LL'}\delta_{ll'}\delta_{mm'} \tag{A4}$$

and

$$\int T_{jk}^{\lambda\, L,lm}\ T_{jk}^{\lambda'\, L',l'm'*} d\Omega = \delta_{\lambda\lambda'}\delta_{LL'}\delta_{ll'}\delta_{mm'}. \tag{A5}$$

Using these harmonics, the four-dimensional wave equation (4) becomes a radial wave equation for a solution $\phi_{l'}(r,t)$ of orbital angular momentum l':

$$-\partial_t^2\phi_{l'}(r,t) + \frac{1}{r}\partial_r^2[r\phi_{l'}(r,t)] - \frac{1}{r^2}l'(l'+1)\phi_{l'}(r,t) = 0. \tag{A6}$$

We use a powerful notational device due to Burke[14] to express these solutions without requiring harmonic decomposition in time and use of spherical Bessel functions. Solutions to (A6) are written in a functional form

$$\phi_{l'}(r,t) = \{\mathcal{F}^{(k)}(t-\epsilon r)\}_{l'}, \tag{A7}$$

where the curly bracket indicates a sum of terms involving powers of r along with derivatives of the function $\mathcal{F}$, which depends only on advanced or retarded time. In (A7), k is the highest derivative of $\mathcal{F}$ with respect to $x = t - \epsilon r$ that appears, l' is the orbital angular momentum of the solution, and ϵ is $+1$ for outgoing and -1 for ingoing solutions. The zero angular momentum solution is

$$\{\mathcal{F}^{(0)}(t-\epsilon r)\}_0 = \frac{1}{r}\mathcal{F}(t-\epsilon r). \tag{A8}$$

Solutions of higher angular momentum are generated through successive applications of a raising operator

$$D_{l'}{}^{+} = \partial_r - l'/r. \tag{A9}$$

using the identity

$$D_{l'}{}^{+}\{\mathcal{F}^{(k)}(t-\epsilon r)\}_{l'} = -\epsilon\{\mathcal{F}^{(k+1)}(t-\epsilon r)\}_{l'+1}. \tag{A10}$$

For example, we then have as the next three solutions

$$\{\mathcal{F}^{(1)}(x)\}_1 = \frac{1}{r}\mathcal{F}^{(1)}(x) + \epsilon\frac{1}{r^2}\mathcal{F}(x), \tag{A11}$$

$$\{\mathcal{F}^{(2)}(x)\}_2 = \frac{1}{r}\mathcal{F}^{(2)}(x) + 3\epsilon\frac{1}{r^2}\mathcal{F}^{(1)}(x) + 3\frac{1}{r^3}\mathcal{F}(x), \tag{A12}$$

$$\{\mathcal{F}^{(3)}(x)\}_3 = \frac{1}{r}\mathcal{F}^{(3)}(x) + 6\epsilon\frac{1}{r^2}\mathcal{F}^{(2)}(x) + 15\frac{1}{r^3}\mathcal{F}^{(1)}(x) + 15\epsilon\frac{1}{r^4}\mathcal{F}(x), \tag{A13}$$

where $x = t - \epsilon r$. The corresponding angular momentum lowering operator,

$$D_{l'}{}^{-} = \partial_r + (l'+1)/r, \tag{A14}$$

when operating on radial solutions, yields lower-order solutions:

$$D_{l'}{}^{-}\{\mathcal{F}^{(k)}(x)\}_{l'} = -\epsilon\{\mathcal{F}^{(k+1)}(x)\}_{l'-1}. \tag{A15}$$

Burke's functionals can be simply related to the more standard basis functions. Following Thorne[3] we similarly denote spherical Hankel functions with the somewhat unusual notation

$$h_{\epsilon l'}(x) = j_{l'}(x) + i\epsilon y_{l'}(x), \tag{A16}$$

where $j_{l'}(x)$ and $y_{l'}(x)$ are the spherical Bessel functions of the first and second kind. In the Burke notation, the Hankel functions can be written as

$$h_{\epsilon l'}(x)=(-i\epsilon)^{l'+1}\{e^{i\epsilon x}\}_{l'}. \tag{A17}$$

It is also possible to express the Burke functional of an arbitrary function $\mathcal{F}(x)$ in terms of Hankel functions. If we take the Fourier transform of $\mathcal{F}(x)$ and take the angular momentum l' bracket of that, we get

$$\{\mathcal{F}(x)\}_{l'}=\frac{1}{(2\pi)^{1/2}}\int_{-\infty}^{\infty}d\omega\, f(\omega)\, e^{-i\omega t}\{e^{i\epsilon\omega r}\}_{l'}. \tag{A18}$$

We can take the inverse Fourier transform to solve for $f(\omega)$ and plug back into (A18). Using (A17) we obtain

$$\{\mathcal{F}(x)\}_{l'}=\frac{1}{2\pi}(-i\epsilon)^{l'+1}\int_{-\infty}^{\infty}d\omega\, e^{-i\omega t}h_{\epsilon l'}(\omega r)\times\int_{-\infty}^{\infty}dx'\,\mathcal{F}(x')\,e^{i\omega x'}. \tag{A19}$$

There are additional connections between the Burke functionals and the Bessel and Hankel functions. Following (A10), the Rodrigues formula has an analogue:

$$\{\mathcal{F}^{(l)}\}_l=(-\epsilon)^l D^+_{l-1}D^+_{l-2}\cdots D^+_1 D^+_0\{\mathcal{F}\}_0. \tag{A20}$$

There is also an algebraic recursion formula for the Burke brackets:

$$\{\mathcal{F}^{(1)}\}_{l+1}+\{\mathcal{F}^{(1)}\}_{l-1}=\frac{2l+1}{r}\epsilon\{\mathcal{F}\}_l. \tag{A21}$$

A final useful relation is

$$(2l+1)\partial_r\{\mathcal{F}\}_l=-\epsilon[(l+1)\{\mathcal{F}^{(1)}\}_{l+1}+l\{\mathcal{F}^{(1)}\}_{l-1}]. \tag{A22}$$

The usual normalization of the pure-orbit harmonics (A4) and (A5) is somewhat inconvenient when a simple result is desired for the components in terms of trigonometric functions or Legendre polynomials. Accordingly we introduce a simple scaling for the vector harmonics:

$$\tilde{\mathbf{Y}}^{l',lm}=c_{l'l}\mathbf{Y}^{l',lm}, \tag{A23a}$$

with

$$c_{l-1,l}=c_{l,l-1}=\left[\frac{4\pi}{l}\right]^{1/2},\qquad c_{l,l}=i\left[\frac{4\pi l(l+1)}{2l+1}\right]^{1/2}, \tag{A23b}$$

and similarly for the tensor harmonics:

$$\tilde{\mathbf{T}}^{\lambda\, l',lm}=d_{\lambda l',l}\mathbf{T}^{\lambda\, l',lm}, \tag{A24a}$$

with

$$d_{0l,l}=-\left[\frac{12\pi}{2l+1}\right]^{1/2}, \tag{A24b}$$

$$d_{2l-2,l}=\left[\frac{4\pi(2l-1)}{(l-1)l}\right]^{1/2}, \tag{A24c}$$

$$d_{2l-1,l}=-i\left[\frac{2\pi l(l+1)}{l-1}\right]^{1/2}, \tag{A24c}$$

$$d_{2l,l}=-\left[\frac{6\pi(2l-1)(2l+3)}{l(l+1)(2l+1)}\right]^{1/2}, \tag{A24c}$$

$$d_{2l+1,l}=i\left[\frac{2\pi l(l+1)}{l+2}\right]^{1/2}, \tag{A24d}$$

$$d_{2l+2,l}=\left[\frac{4\pi(2l+3)}{(l+1)(l+2)}\right]^{1/2}. \tag{A24d}$$

In performing infinitesimal gauge transformations it is useful to have expressions for the action of the Killing operator [Eq. (25)] on a general term: a radial function multiplied by a vector harmonic. Using expressions in Mathews[35] or Edmonds,[34] one can derive

$$[K(\Phi\tilde{Y}^{l-1,lm})]_{ij}=2\left[\frac{l-1}{2l-1}\right]D^-_{l-1}\Phi\tilde{T}^{2\,l-2,lm}_{ij}+\left[\frac{2(l+1)}{3(2l-1)}\right]D^+_{l-1}\Phi\tilde{T}^{2\,l,lm}_{ij}+\tfrac{2}{3}D^+_{l-1}\Phi\tilde{T}^{0\,l,lm}_{ij}, \tag{A25a}$$

$$[K(\Phi\tilde{Y}^{l,lm})]_{ij}=-\left[\frac{2(l-1)}{2l+1}\right]D^-_{l}\Phi\tilde{T}^{2\,l-1,lm}_{ij}-\left[\frac{2(l+2)}{2l+1}\right]D^+_{l}\Phi\tilde{T}^{2\,l+1,lm}_{ij}, \tag{A25b}$$

$$[K(\Phi\tilde{Y}^{l+1,lm})]_{ij}=-\frac{2}{3}\frac{l}{2l+3}D^-_{l+1}\Phi\tilde{T}^{2\,l,lm}_{ij}-2\left[\frac{l+2}{2l+3}\right]D^+_{l+1}\Phi\tilde{T}^{2\,l+2,lm}_{ij}-\tfrac{2}{3}D^-_{l+1}\Phi\tilde{T}^{0\,l,lm}_{ij}. \tag{A25c}$$

[1]R. Arnowitt, S. Deser, and C. W. Misner, in *Gravitation: An Introduction to Current Research,* edited by L. Witten (Wiley, New York, 1962).

[2]J. W. York, Jr., in *Sources of Gravitational Radiation,* edited by L. L. Smarr (Cambridge University Press, Cambridge, England, 1979).

[3]K. S. Thorne, Rev. Mod. Phys. **52**, 299 (1980).

[4]C. R. Evans, in *Dynamical Spacetimes and Numerical Relativity,* edited by J. Centrella (Cambridge University Press, Cambridge, England, 1986).

[5]D. M. Eardley, in *Sources of Gravitational Radiation* (Ref. 2).
[6]J. M. Stewart, in *Astrophysical Radiation Hydrodynamics,* edited by M. L. Norman and K-H. A. Winkler (Reidel, Dordrecht, 1986); R. A. Isaacson, J. S. Welling, and J. Winicour, J. Math. Phys. **24**, 1824 (1983).
[7]L. Smarr, in *Sources of Gravitational Radiation* (Ref. 2), p. 245.
[8]L. Smarr and J. W. York, Jr., Phys. Rev. D. **17**, 1945 (1978); **17**, 2529 (1978).
[9]J. M. Bardeen, in *Gravitational Radiation,* edited by N. Dereulle and T. Piran (North-Holland, Amsterdam, 1983).
[10]B. F. Schutz, in *Dynamical Spacetimes and Numerical Relativity* (Ref. 4).
[11]J. M. Bardeen and T. Piran, Phys. Rep. **96**, 205 (1983).
[12]J. Anderson and D. Hobill, in *Dynamical Spacetimes and Numerical Relativity* (Ref. 4).
[13]C. W. Misner, K. S. Thorne, and J. A. Wheeler, *Gravitation* (Freeman, San Francisco, 1973).
[14]W. L. Burke, J. Math. Phys. **12**, 401 (1971).
[15]S. A. Teukolsky, Phys. Rev. D **26**, 745 (1982).
[16]See Thorne (Ref. 3), Secs. II.E and IV.A; our $\mathcal{I}_{lm}$ and $\mathcal{S}_{lm}$ in Eq. (12) are equivalent to his I^{lm} and S^{lm} in his Eq. (4.3).
[17]This solution is essentially a generalization of the quadrupole solution found in Teukolsky (Ref. 15). It is equivalent to the solution given by Thorne (Ref. 3) [his Eqs. (8.12) and (8.13)] in STF notation and translated here into pure-orbit harmonic notation.
[18]Schutz (Ref. 10) has pointed out that matched analytic-numerical techniques may be crucial for three-dimensional codes because of computer resource limitations.
[19]Our $l=3$ current moment satisfies equatorial plane symmetry, as opposed to Teukolsky's $l=2$ odd-parity solution (Ref. 15).
[20]We will for brevity subsequently refer to these as the quadrupole and octupole moments, though the strictly proper use of these terms refer to $\mathcal{I}_{20}$ and $\mathcal{S}_{30}$.
[21]See Bardeen in Ref. 9, his Eq. (9). Correspondence is made between our expressions and Teukolsky's (Ref. 15) notation by the identification $I=\frac{3}{4}F^{(2)}$. Note Bardeen's sign difference and the typographical error in the third term of his Eq. (9). This result can also be obtained from our Eq. (66).
[22]The integration constants are discussed in Sec. V, which ascribes them to arbitrariness in gauge.
[23]York in Ref. 2, p. 117 discusses the idea of using harmonic coordinates in a numerical scheme and the potential interpretive problems.
[24]D. M. Eardley and L. Smarr, Phys. Rev. D. **19**, 2239 (1979).
[25]D. M. Eardley, talk given at meeting on Numerical Astrophysics at the University of Illinois, 1982 (unpublished); Bardeen and Piran (Ref. 11), Sec. 5.2.
[26]C. R. Evans, Ph.D. thesis, University of Texas at Austin, 1984.
[27]J. R. Wilson, in *Sources of Gravitational Radiation* (Ref. 2).
[28]Bardeen (Ref. 9) has also given the transformation for the mass quadrupole $l=2$ solution to QI gauge, though truncated at $O(r^{-5})$.
[29]Bardeen (Ref. 9) in contrast expands the integral in inverse powers of r and truncates the expansion at $O(r^{-5})$. Such an expansion would present difficulties to matching in the near zone where $\lambda\!\!\!^{-}/r \gtrsim 1$.
[30]L. S. Finn, in Gravitational Wave Data Analysis, edited by B. F. Schutz (Reidel, Dordrecht, to be published).
[31]Like the gauge term b_2, the mass M obtained from Eq. (54) should be independent of radius and very nearly constant in time. Past experience with other quasilocal mass measures indicates that this can be achieved numerically to fractional errors of less than 10^{-4}.
[32]L. Smarr (private communication).
[33]R. F. Stark and T. Piran, in *Proceedings of the Fourth Marcel Grossman Meeting on General Relativity,* Rome, Italy, 1985, edited by R. Ruffini (North-Holland, Amsterdam, 1986); see their Fig. 9.
[34]A. R. Edmonds, *Angular Momentum in Quantum Mechanics* (Princeton University Press, Princeton, 1974).
[35]J. Mathews, *Tensor Spherical Harmonics* (Caltech Graphics Arts, Pasadena, 1981).
[36]F. J. Zerilli, J. Math. Phys. **11**, 2203 (1970).